



Research paper

Photoinactivation of microorganisms with sub-micromolar concentrations of imidazolium metallophthalocyanine salts

Rafael T. Aroso^a, Mário J.F. Calvete^{a, **}, Barbara Pucelik^{b, c}, Grzegorz Dubin^c,
Luis G. Arnaut^a, Mariette M. Pereira^a, Janusz M. Dąbrowski^{b, *}

^a CQC, Department of Chemistry, University of Coimbra, 3004-535, Coimbra, Portugal

^b Faculty of Chemistry, Jagiellonian University, Gronostajowa 2, 30-387, Kraków, Poland

^c Malopolska Centre of Biotechnology, Jagiellonian University, Gronostajowa 7A, 30-387, Kraków, Poland

ARTICLE INFO

Article history:

Received 21 June 2019

Received in revised form

25 September 2019

Accepted 25 September 2019

Available online 28 September 2019

Keywords:

Photodynamic inactivation of

microorganisms (PDI)

Multidrug resistance (MDR)

Phthalocyanines

Photosensitizing drugs

Reactive oxygen species (ROS)

Imidazolium phthalocyanine salts

ABSTRACT

The increasingly limited therapeutic options for the treatment of infections caused by multi-resistant Gram-negative bacteria due to the alarming increase in bacteria resistance, renewed interest in photodynamic inactivation (PDI) of bacteria. We address PDI of multi-resistant bacteria with a new family of cationic tetra-imidazolyl phthalocyanines bearing a diversity of cationizing alkyl chain sizes, degrees of cationization and coordinating metals. The antimicrobial activities of the phthalocyanines under white light against Gram-positive and Gram-negative bacteria have remarkable differences in efficacy. We relate their spectroscopic and photophysical properties with the generation of reactive oxygen species (ROS), biological performance and structural features. We show that sub-micromolar concentrations of a Zn(II) tetra-ethyl cationic phthalocyanine reduce colonies of Gram-negative bacteria (*E. coli*, *P. aeruginosa*) and *C. albicans* by 7 log units while leaving mammalian cells unharmed. This is a new lead to address hard-to-treat localized infections.

© 2019 The Authors. Published by Elsevier Masson SAS. This is an open access article under the CC BY license (<http://creativecommons.org/licenses/by/4.0/>).

1. Introduction

The increase of bacteria multi-drug resistance is becoming a major social threat and a growing economic burden to healthcare systems [1]. According to a recent WHO report [2,3], the number of infection-related deaths caused by multi-resistant microorganisms is likely to steadily increase and is projected to reach 10 million deaths/year worldwide by 2050. New classes of antibiotics effective against Gram-positive bacteria were recently discovered [4], but

progress regarding control of infections by Gram-negative bacteria is unsatisfactory [5]. Moreover, the increasing ability of bacteria to acquire resistance to conventional antibiotics, especially when they have one single target in the cell, recommends exploring therapeutic approaches that are less prone to resistance [6,7]. Among them, photodynamic inactivation (PDI) of bacteria [8–12] has already provided good examples of efficient inactivation of multi-drug resistant strains of *S. aureus*, *P. aeruginosa*, *E. coli* and *A. baumannii* [13,14]. PDI combines a photosensitizer molecule, a light source and molecular oxygen to generate reactive oxygen species (ROS), namely $^1\text{O}_2$, $\text{O}_2^{\bullet-}$, H_2O_2 and HO^{\bullet} . These ROS produce oxidative stress in microorganisms that trigger various mechanisms of action eventually leading to cell death [11,15–18]. PDI is a multi-targeted approach because ROS react with a wide range of biomolecules. In particular, singlet oxygen generated inside a bacterium can explore all of its size and react anywhere in the cell [19]. It is now accepted that, compared to classical antibiotic therapies, PDI-treated bacteria are less prone to development of multidrug resistance (MDR) [15,20–23].

It is recognized that Gram-positive bacteria are more susceptible to PDI, but the factors that govern that susceptibility are not yet

Abbreviations: APF, 3'-(p-aminophenyl) fluorescein; CFU, colony forming unit; CLSM, confocal laser scanning microscopy; DHE, dihydroethidium; DMAE, dimethylaminoethanol; DMF, N,N-dimethylformamide; DMSO, dimethyl sulfoxide; HBSS, Hank's balanced salt solution; HPF, 3'-(p-hydroxyphenyl) fluorescein; MTT, 3-(4,5-Dimethylthiazol-2-yl)-2,5-diphenyltetrazolium bromide; PBS, phosphate buffered saline; PDI, photodynamic inactivation; PS, photosensitizer; ROS, reactive oxygen species; SOSG, Singlet Oxygen Sensor Green; Φ_{Δ} , singlet oxygen quantum yield; Φ_F , fluorescence quantum yield.

* Corresponding author.

** Corresponding author.

E-mail addresses: mcalvete@qui.uc.pt (M.J.F. Calvete), jdabrows@chemia.uj.edu.pl (J.M. Dąbrowski).

clearly understood [11]. The understanding of such factors may guide the design and development of better antimicrobial photosensitizers, capable of inactivating Gram-positive bacteria and also the very challenging Gram-negative bacteria. Gram-negative bacteria that are amongst the most frequent cause of nosocomial infections and of infections in immunosuppressed patients [24]. The difficulty to kill Gram-negative bacteria is largely due to presence of an outer membrane that serves as a highly impermeable barrier to antibiotics. The presence of lipopolysaccharides in the outer membrane of Gram-negative bacteria may also induce the release of pro-inflammatory cytokines from host cells and can act as a potent virulence factor. Another important virulence factor is the ability to secrete proteases which can degrade the matrix proteins impairing tissue integrity as well as disrupt defence systems such as antibodies or cytokines [24]. Moreover, many of Gram-negative bacteria (e.g. *P. aeruginosa*) contain endotoxins that are able to block potential drugs and protect the sensitive inner membrane and cell wall [25]. Rationally designed photosensitizers may contribute to surmount these obstacles and overcome drug-resistance mechanisms of traditional antibiotic therapy [20,26].

Phthalocyanines were shown to be efficient photosensitizers in the photodynamic inactivation of microorganisms [12] as well as in photodynamic therapy of cancer [27]. Cationization and metalation of photosensitizers improved PDI of microorganisms [7,28,29]. For instance, cationic zinc pyridinium phthalocyanine [30] and cationic N-methylpyridinium porphyrins [31] were among the examples of photosensitizers capable of photoinactivating both Gram-negative and Gram-positive bacteria. These pioneer studies helped to realize that effective PDI of Gram-negative bacteria required a photosensitizer with a pronounced cationic charge. The quest for cationic photosensitizers with stronger light absorption in the near-infrared motivated the development of cationic chlorins [32,33], bacteriochlorins [34,35], porphycenes [36] and phthalocyanines [37,38], and the characterization of their PDI effect. Zn(II) cationic anilinium phthalocyanines are among the best examples of cationic metallophthalocyanines: 0.1 μM concentrations and 5 min irradiation with 600–700 nm light (50 mW/cm²) led to a 5 logs reduction of *S. aureus* colonies [39]. Although the inactivation of Gram-negative bacteria is more challenging, PDI using phthalocyanines with different structural motifs were reported [40–48]. Dei et al. used cationic phthalocyanines bearing trialkylammonium groups and were able to reduce *E. coli* colonies by 6 log units with 1 μM photosensitizer concentration and red light irradiation (50 mW/cm²) for 10 min [49]. Cationic phthalocyanines can also inactivate fungi [50–53]. The family of phthalocyanines mentioned above achieved a 6 log reduction of *C. albicans* at photosensitizer concentrations of 1 μM under red light irradiation (50 mW/cm²) for 10 min [49].

A good disinfection consists in decreasing the number of bacteria colonies by 5 or 6 log units. The photosensitizers currently employed in PDI require micromolar concentrations to meet this goal [54]. Attempts to increase the potency of phthalocyanines for PDI should consider the following factors: i) adding cationic groups to increase electrostatic interaction with the outer membrane improves PDI of Gram-negative bacteria and increases hydrophilicity [8,49]; ii) increasing of the size of cationizing alkyl chain favours photosensitizer uptake [50] and may result in enhanced antimicrobial activity [55,56]. The role of differences in cell wall thickness between Gram-positive and Gram-negative bacteria (20–80 nm for Gram-positive bacteria and 10–15 nm for Gram-negative species) was investigated using crystal violet-based photosensitizers. The depth of the modified derivative in the bacterial cell walls plays a key role in its PDI selectivity, which in turns is controlled by the positive charges of the photosensitizer [57]. It must be realized that PDI *in vivo* adds the problem that increased phototoxicity is often

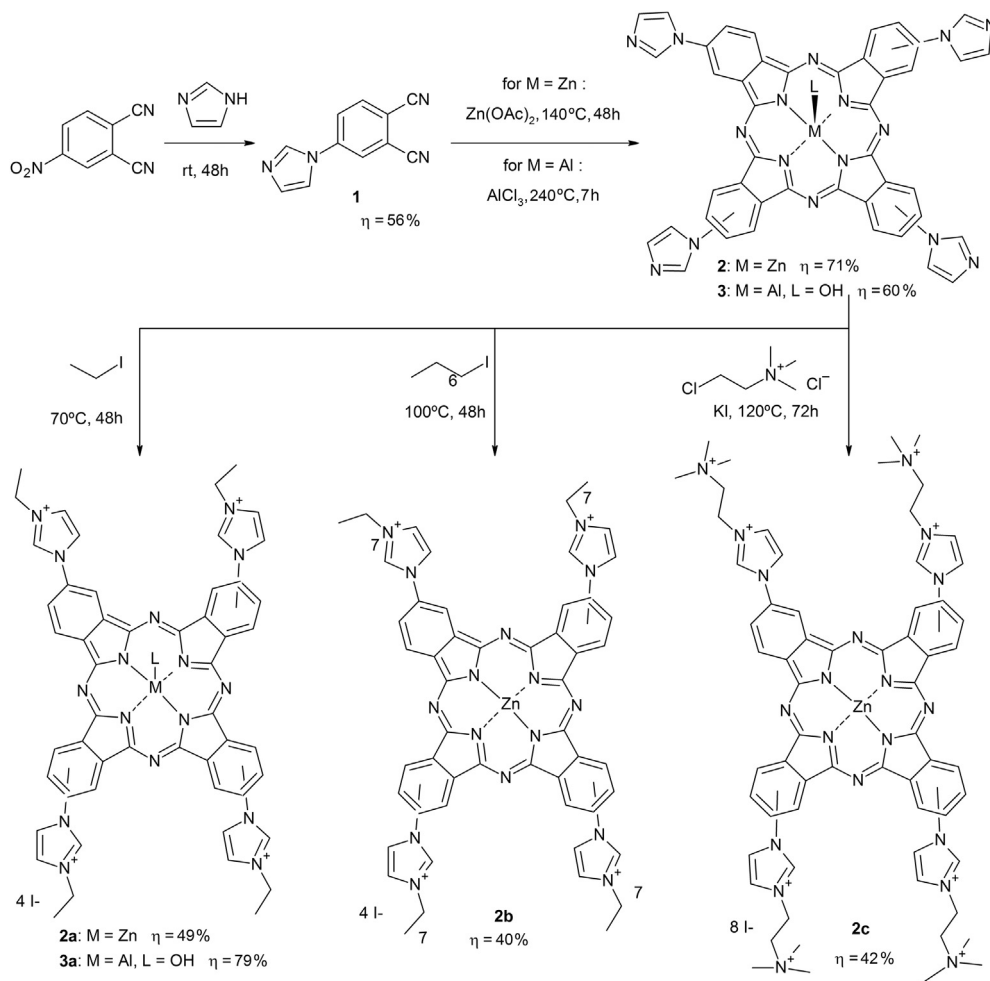
correlated with damage to normal tissue [58], and is still unclear how to favour PDI of microorganisms without phototoxicity towards human cells. Structure-activity relationships and formulations for PDI must also consider cytotoxicity towards eukaryotic cells.

It came to our attention that imidazole-containing metallophthalocyanines showed good photosensitizing results towards cancer cells [59], but their use in PDI of bacteria was overlooked. We decided to synthesise a new family of imidazole-substituted Zn(II) and Al(III) phthalocyanines with a different number of positive charges and cationizing alkyl chain of different lengths. We studied the influence of these structural modifications on uptake and PDI of microbial cells, as well as their toxicity towards human cells. The photosensitizers photophysical and photochemical properties, and their ROS generation efficacy in biological media were characterized. Their uptake was also investigated by confocal laser scanning microscopy and correlated with PDI activity. We succeeded, for the first time, to reduce by 7 logs units the number of colonies of two Gram-negative bacteria (*E. coli* and *P. aeruginosa*) using nanomolar photosensitizer concentrations under conditions of negligible phototoxicity towards human cells.

2. Results and discussion

Synthesis. The cationic phthalocyanines used in this study were synthesized according to Scheme 1. 4-(1H-imidazol-1-yl)phthalonitrile **1** was prepared by reacting commercial 4-nitrophthalonitrile with imidazole in DMF, at room temperature, in the presence of K₂CO₃, and was isolated in 56% yield. The cyclotetramerization reaction of phthalonitrile **1** and Zn(II) acetate was performed in dimethylaminoethanol (DMAE) at 140 °C for 48 h. The corresponding Al(III) phthalocyanine, was obtained by adding AlCl₃ to phthalonitrile **1** in 1-chloronaphthalene and reacting at 240 °C for 6 h. After precipitation of the product from the reaction medium and purification by consecutive washing using solvents with increasing polarities (dichloromethane, acetone, methanol and water), the corresponding tetra-imidazole β -substituted metallophthalocyanines **2** and **3** were isolated in 71% and 60% yields, respectively. The products, and in particular **2**, showed poor solubility in most organic solvents, except in DMF, DMSO and pyridine. This is likely to be caused by π - π stacking. However, compounds **2** and **3** were readily soluble in protic solvents at acidic pH, as expected, given the basic properties of imidazole group. Satisfactory ¹H NMR spectra of non-protonated dye **2** could only be obtained in pyridine-d₅ at 80 °C, as previously described for other planar phthalocyanines [60].

Reaction of **2** with iodoethane or iodoctane in DMF yielded tetra-cationic Zn(II) phthalocyanines with varied degrees of lipophilicity, **2a** and **2b**, respectively, which were isolated by direct precipitation from the reaction mixture by adding CH₂Cl₂ or diethyl ether, respectively. The octa-cationic phthalocyanine **2c** was obtained by reaction of **2** with commercial (2-chloroethyl)trimethylammonium chloride. This strategy improved significantly the synthesis of octa-cationic phthalocyanines, when compared with an earlier report involving synthetically demanding routes [44,49]. Compared with **2a** and **2b**, the synthesis of **2c** required the use of potassium iodide as catalyst and increased reaction time and temperature, to overcome for lower reactivity of the chloroalkylammonium salt. The crude product was obtained by direct precipitation from the reaction mixture with CH₂Cl₂, followed by washing with ethanol. Further purification using gel permeation chromatography ensured the removal of the unreacted ionic reagent. The ¹H NMR spectrum of **2c** in DMSO-d₆ showed small broad signals, regardless of its concentration and addition of D₂O, which were ascribed to aggregation. Elemental analysis indicated traces of



Scheme 1. Synthetic procedure used to obtain the cationic Zn(II) and Al(III) phthalocyanines.

catalyst, but further purification was not attempted, given recent reports on KI mediated enhancement of PDI [61]. Al(III) tetra-ethyl cationic phthalocyanine **3a** was synthesized by reacting **3** with iodoethane using a protocol identical to that used to obtain **2a**.

Electronic absorption and emission measurements. All the metallophthalocyanines showed UV–Vis spectra in DMSO typical of this class of compounds in monomeric form, with a Soret band (300–400 nm) and a Q band centred at 682 nm for **2**, 677 nm for **2a–c**, 693 nm for **3** and 680 nm for **3a** which also showed a satellite

band corresponding to a vibronic transition (Fig. 1a and b). The blue shift of **2a–c** relative to **2** is likely to result from the reduced electron-donating ability of the quaternized imidazole group. Absorption spectra in H₂O revealed different extents of aggregation. The polar axial ligand OH in **3a** seems to prevent aggregation because the spectra in water and DMSO are almost identical and characteristic for monomeric species. The spectrum of octa-cationic phthalocyanine **2c** in H₂O shows a small increase of the 612 nm band, a consequence of exciton coupling due to formation of dimers

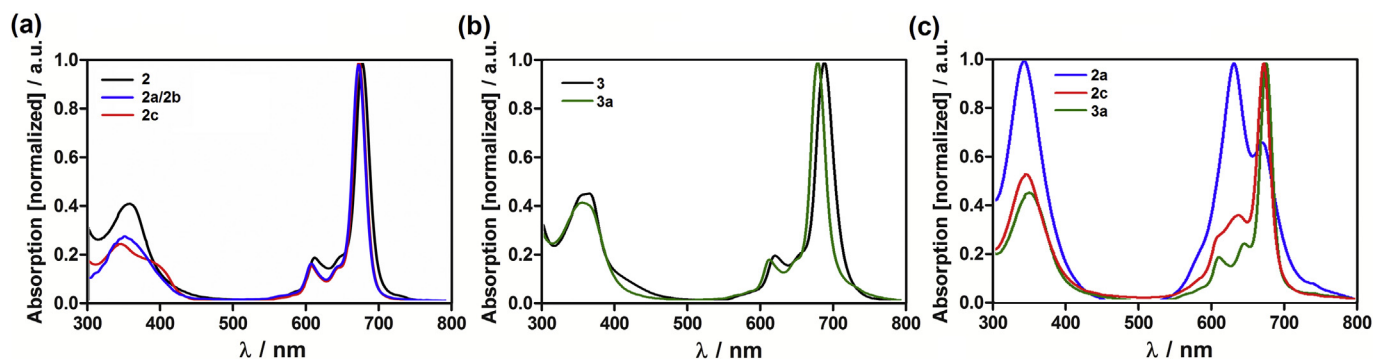


Fig. 1. Normalized UV–Vis absorption spectra. (a) Zn(II) metallophthalocyanines (**2** and **2a–c**) in DMSO; (b) Al(III) metallophthalocyanines (**3** and **3a**) in DMSO; (c) water-soluble cationic metallophthalocyanines (**2a**, **2c** and **3a**) in H₂O.

in solution [60]. On the other hand, the 616 nm band of **2a** is significantly increased, revealing more extensive aggregation. The electrostatic repulsion between positively charged moieties in **2c** is effective in reducing π - π stacking. Data for **2b** is not provided because its solubility in aqueous media is too low to obtain meaningful spectra, as expected from its increased lipophilicity. The absorption coefficients of the bands are summarized in Table 1 and are typical for metallophthalocyanines [27,62,63].

The fluorescence spectra of these phthalocyanines in DMSO is characterized by intense bands with maxima at 691 nm for **2**, 687 nm for **2a-c**, 702 nm for **3** and 691 nm for **3a** which also has small vibronic band. The fluorescence is a good mirror image of the absorption as expected for rigid and planar macrocycles with negligible structural changes between ground and excited singlet states.

Fluorescence excitation spectra in DMSO are similar to the corresponding absorption spectra. This corroborates the absence of contamination with free-base phthalocyanines in our samples. However, the fluorescence excitation and absorption of water-soluble phthalocyanines, recorded in aqueous media, showed marked differences (Fig. 2b). No fluorescence emission was associated with absorption band at 630–640 nm. This corroborates the assignment of this band to dimers. The fluorescence excitation peak corresponds to the absorption band at 677 nm, assigned to the monomer, which means only monomeric species are fluorescent in solution. This is expected because radiative decay of the dimers from their lowest energy excited state to the ground state is a forbidden transition. All Zn(II) and Al(III) metal complexes have moderate values of Φ_F , which is in accordance to the values obtained by other authors [62].

Singlet oxygen generation. Singlet oxygen is one of the most significant PDI effectors. Its production relies, among other factors, on the ability of the photosensitizer to intersystem crossing from the singlet excited state, prepared by electronic excitation, to a long-lived triplet state. Diamagnetic metal complexes, namely those with Zn(II) and Al(III), do not have metal-to-ligand charge transfer states with energies between the HOMO and LUMO of the macrocycles that could quickly deactivate ligand π, π^* states. Moreover, Al(III) and, especially, Zn(II) provide internal heavy-atom effects that accelerate intersystem crossing to the triplet state. Hence, by design, these complexes can have long-lived triplet states formed with high quantum yields, which are ideal for singlet oxygen generation [65].

Singlet oxygen quantum yields were determined in DMSO using time-dependent singlet oxygen phosphorescence emission at 1270 nm (Table 2). ZnPc ($\Phi_\Delta = 0.67$) was used as standard [64]. As expected [66], all zinc metallophthalocyanines have high Φ_Δ values, while the aluminium complexes have markedly lower Φ_Δ . The intermediate yield of compound **2** is likely a consequence of its aggregation in the DMSO.

ROS generation in aqueous medium. The generation of other

ROS, most notably hydroxyl radicals, was evaluated in aqueous medium using aminophenyl fluorescein (APF), hydroxyphenyl fluorescein (HPF) and dihydroethidium (DHE) (Fig. 3) [54]. Singlet oxygen sensor green (SOSG) was also employed for comparison with singlet oxygen phosphorescence measurements.

Using APF and HPF as measures of hydroxyl radical generation, compound **2b** was the most efficient generator of hydroxyl radicals (Fig. 3a and b). Taking the redox-sensitive probe DHE as a measure of the relative generation of superoxide ions (Figure 3d), **2b** was the least efficient in this regard. Singlet oxygen sensor green was less discriminative than singlet oxygen phosphorescence to rank the efficiency in singlet oxygen generation (Fig. 3c), but **3a** yielded the lowest amount of singlet oxygen, consistent with Table 2.

The response of the fluorescent probes suggests that these phthalocyanines are likely to undergo both Type I and Type II mechanisms. Singlet oxygen quantum yields are highest for **2b**, but its ability to generate ROS that oxidize DHE is the lowest. Interestingly, **3a** has the opposite behaviour: it is the worst generator of singlet oxygen but induced the highest fluorescence of DHE. Cationic photosensitizers are expected to interact strongly with Gram-negative. It is likely that tightly bound photosensitizers generate larger amount of ROS leading to more efficient killing. A word of caution must be said on the possible dependence of the photochemical mechanisms of ROS generation on the biological environment: blood, serum or tissue infection may favour different mechanisms [67].

Log P_{OW} determination. Another factor that contributes to the uptake of a photosensitizer by microbial cells is its lipophilicity, which can be assessed by *n*-octanol:water partition coefficients (P_{OW}). P_{OW} values were obtained using the shake-flask method and are summarized in Table 3 in terms of their logarithmic values (log P_{OW}). The investigated phthalocyanines cover a wide range of lipophilicities. The higher lipophilicity of **2b** is related to its long alkyl chains. This may improve uptake and overall efficiency due to the enhanced interaction with biological membranes. The other photosensitizers are more hydrophilic, especially **2a** which is of smaller size. However, it was shown that photosensitizers do not have to cross the cell envelope of Gram-negative bacteria to be phototoxic [68], since the diffusion length of singlet oxygen in water is longer than the width of the cell envelope [69]. Photosensitizers electrostatically attached to the outer membrane of bacteria may also be efficient PDI photosensitizers.

Photosensitizer uptake by microorganisms. We assessed the uptake of cationic photosensitizers **2a-c** and **3a** by Gram-positive (*E. faecalis* and *S. aureus*) and Gram-negative (*E. coli* and *P. aeruginosa*) bacteria, and fungi (*C. albicans*) (Fig. 4a–e). The long alkyl chains in the cationic phthalocyanine **2b** led to significantly higher uptake in all tested microorganisms, as in earlier work [51,55,56]. This is reflected in the higher log P_{OW} of **2b**. The uptake of **2a** is higher for fungi (*C. albicans*) and for Gram-positive bacteria (*E. faecalis* and *S. aureus*) than for the Gram-negative species (*E. coli*

Table 1
Photophysical properties of metallophthalocyanines determined in DMSO.

Phthalocyanine	Absorption $\epsilon/\text{M}^{-1} \text{ cm}^{-1}$ (λ/nm)	Fluorescence (nm)	Stokes shift (nm)	Φ_F^a
2	– (358), – (616), – (682) ^b	691	9	0.14
2a	$7.4 \cdot 10^4$ (354), $4.4 \cdot 10^4$ (611), $2.8 \cdot 10^5$ (677)	687	10	0.17
2b	$6.2 \cdot 10^4$ (354), $3.7 \cdot 10^4$ (611), $2.4 \cdot 10^5$ (677)	687	10	0.19
2c	$5.5 \cdot 10^4$ (343), $3.6 \cdot 10^4$ (612), $2.6 \cdot 10^5$ (677)	687	10	0.09
3	$7.0 \cdot 10^4$ (364), $3.5 \cdot 10^4$ (624), $1.8 \cdot 10^5$ (693)	702	9	0.30
3a	$7.0 \cdot 10^4$ (357), $3.0 \cdot 10^4$ (616), $1.7 \cdot 10^5$ (680)	691	11	0.23

^a Std. Φ_F (ZnPc) = 0.18 (DMSO) [64]. Values determined in the concentration range of 1.0 – $3.0 \cdot 10^{-6}$ M.

^b Due to low solubility of the compound, no reliable values for ϵ were obtained.

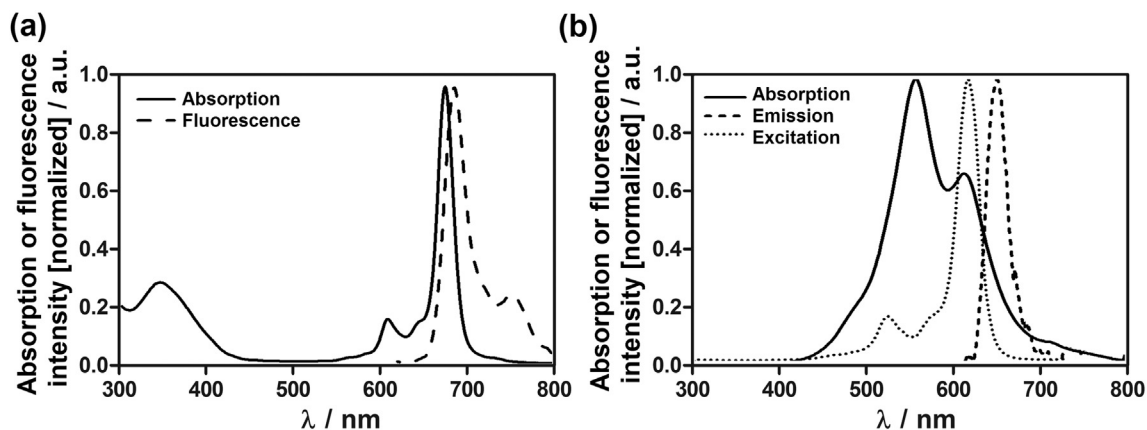


Fig. 2. (a) Example of superposition of absorption and fluorescence emission ($\lambda_{\text{exc}} = 610$ nm) spectra for **2a** in DMSO; (b) Absorption, fluorescence ($\lambda_{\text{exc}} = 610$ nm) and fluorescence excitation spectra of **2a** in H₂O.

Table 2
Singlet oxygen quantum yields (Φ_{Δ}) determined in DMSO.

Phthalocyanine	Φ_{Δ}^a
2	0.56
2a	0.66
2b	0.72
2c	0.67
3	0.33
3a	0.32

^a Std. Φ_{Δ} (ZnPc) = 0.67 (DMSO) [64].

Table 3
Logarithm of partition coefficients ($\log P_{\text{OW}}$) of metallophthalocyanines.

Phthalocyanine	$\log P_{\text{OW}}$
2a	−3.45
2b	1.17
2c	−0.56
3a	−2.34

and *P. aeruginosa*). Replacing Zn^{2+} by $\text{Al}(\text{OH})^{2+}$ in **2a** versus **3a** lowers the uptake significantly. The uptake of **2c** is more complex but its 8 positive charges do not bring an advantage relative to the 4

positive charges of **2a**.

Photodynamic inactivation of microorganisms. PDI with cationic photosensitizers was evaluated against Gram-positive bacteria, Gram-negative bacteria and fungi (Fig. 5a–e). Inactivation with Zn(II) phthalocyanines was more pronounced towards

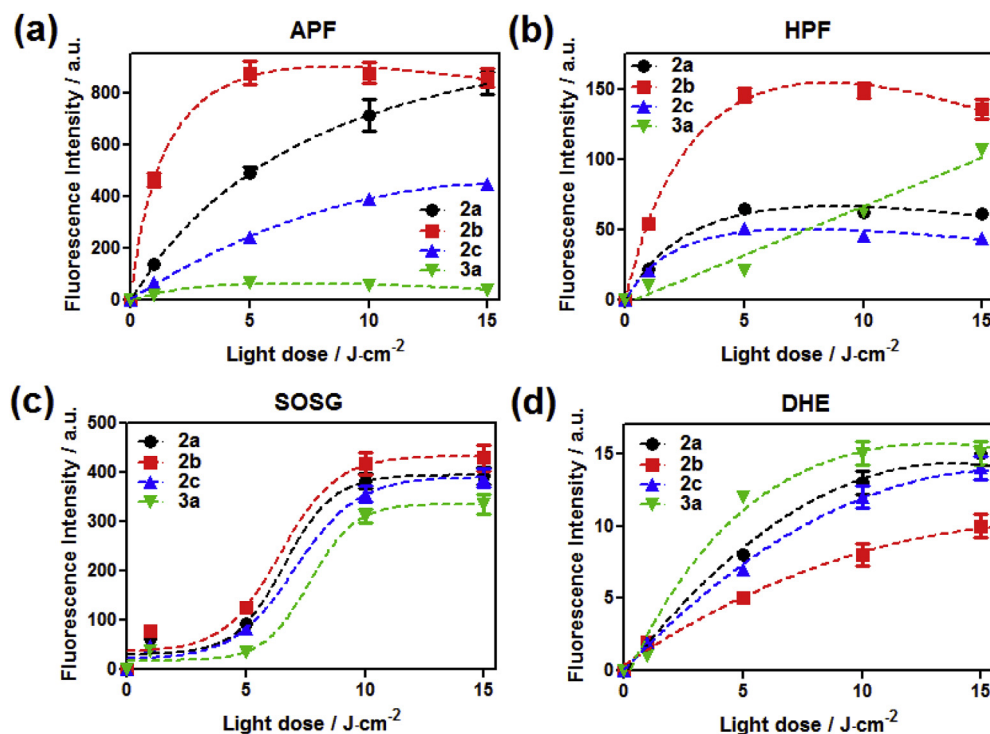


Fig. 3. Detection of reactive oxygen species in biological medium using various ROS probes (25 μM) by irradiation of cationic phthalocyanines (10 μM) with white light in the presence of: (a) 3'-(p-Aminophenyl) fluorescein (APF), (b) 3'-(p-Hydroxyphenyl) fluorescein (HPF), (c) singlet oxygen sensor green (SOSG) and (d) dihydroethidium (DHE). (For interpretation of the references to colour in this figure legend, the reader is referred to the Web version of this article.)

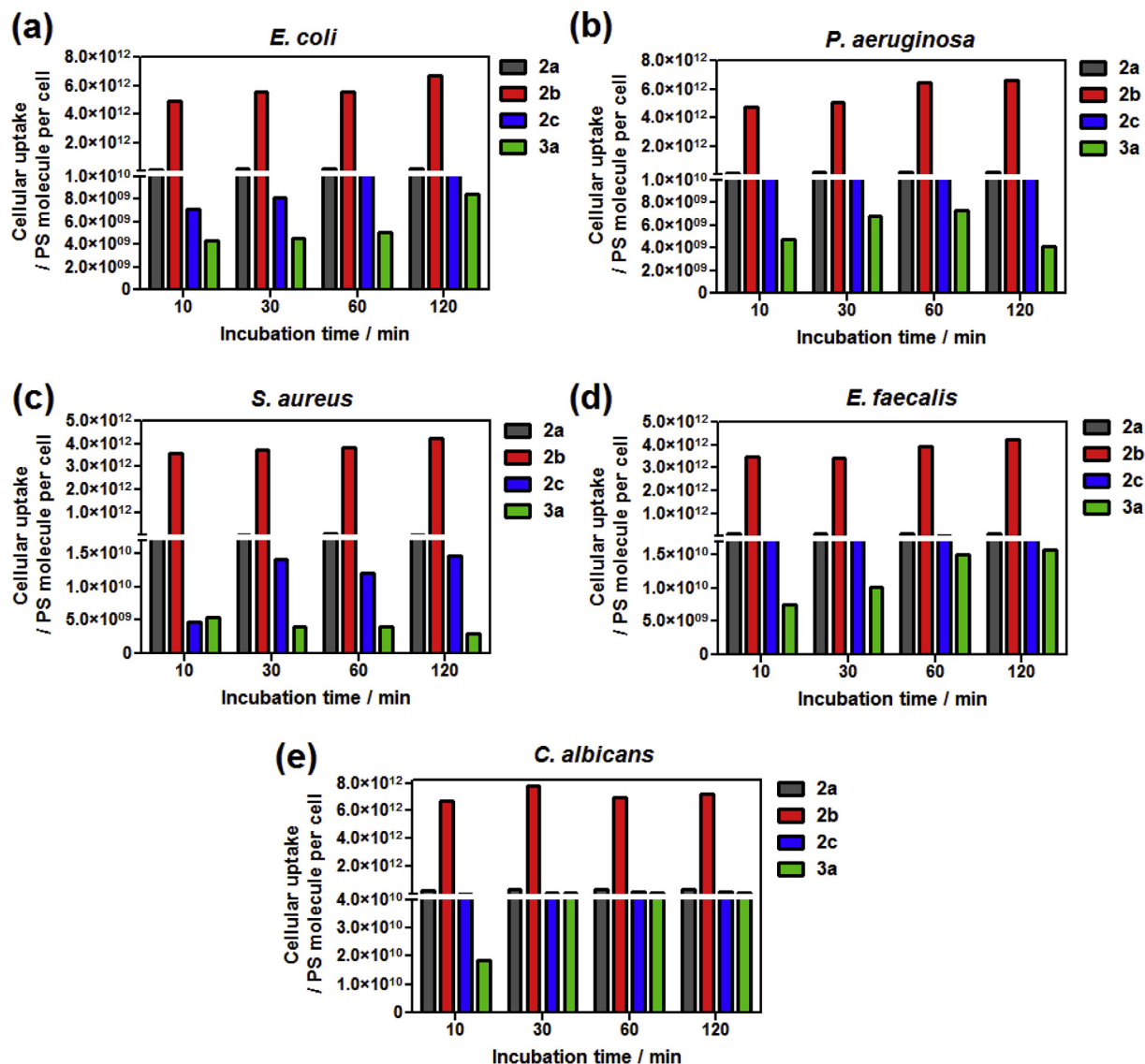


Fig. 4. Uptake of cationic phthalocyanines **2a**, **2b**, **2c** and **3a**: (a) *E. coli*, (b) *P. aeruginosa*, (c) *S. aureus*, (d) *E. faecalis*, (e) *C. albicans*.

Gram negative bacteria. Compound **2a** was particularly effective, enabling a 7 logs reduction in both *E. coli* and *P. aeruginosa* at the lowest concentration tested (100 nM). This is a remarkable PDI efficacy in view of the resistance of Gram-negative bacteria acknowledged in the literature. In fact, it exceeds the 6-log units reduction efficiency targeted in FDA guidelines to ensure a high level of disinfection [70]. The inactivation of Gram-positive bacteria was less noteworthy. However, Al(III) phthalocyanine **3a** proved effective against *S. aureus* although its uptake is particularly low. In fact, we did not find a correlation between uptake and PDI efficacy in this series of photosensitizers: the much higher uptake of the more lipophilic phthalocyanine **2b** did not translate into higher PDI efficacy. A different view was offered in the literature using a series of zinc porphyrins [56]. Our results advise against using uptake as a surrogate of PDI efficacy. Phthalocyanine **2b** has the highest uptake and the highest singlet oxygen quantum yield in DMSO but is less phototoxic than phthalocyanine **2a**.

It is common to report the potency of antibiotics in terms of their minimal inhibitory concentration (MIC). This is less meaningful in PDI because the ability to kill microorganisms comes from the drug and light doses rather than the drug dose alone. Moreover,

the effective light dose depends on the overlap between the spectrum of the light source and the absorption spectrum of the photosensitizers [71]. In view of these limitations, the MIC values reported in Table 4 must be regarded with caution. Nevertheless, it is shown that MIC values for **2a** are as low as those of potent antibiotics.

Various promising photosensitizers for PDI of bacteria and fungi have been reported [7,54,72,73]. Such reports showed that Gram-positive bacteria more susceptible to PDI because their cell wall is more permeable [25]. Fig. 5 shows that **2a** is noteworthy for its higher phototoxic towards Gram-negative bacteria, although it is also very phototoxic to Gram-positive bacteria. This opens new perspectives in the design of novel photosensitizers active against multiple microorganisms. Clinical applications will favour the use of a single photosensitizer that can kill both classes of bacteria, allowing PDI without prior identification of the cause of infectious disease [74]. It is tempting to assign the notable efficacy of **3a** against *S. aureus* to its ability to oxidize DHE. We speculate that some vital structures in *S. aureus* are sensitive to oxidation by the same mechanism as the oxidation of DHE.

Our PDI protocol relies on both soluble and cell bound

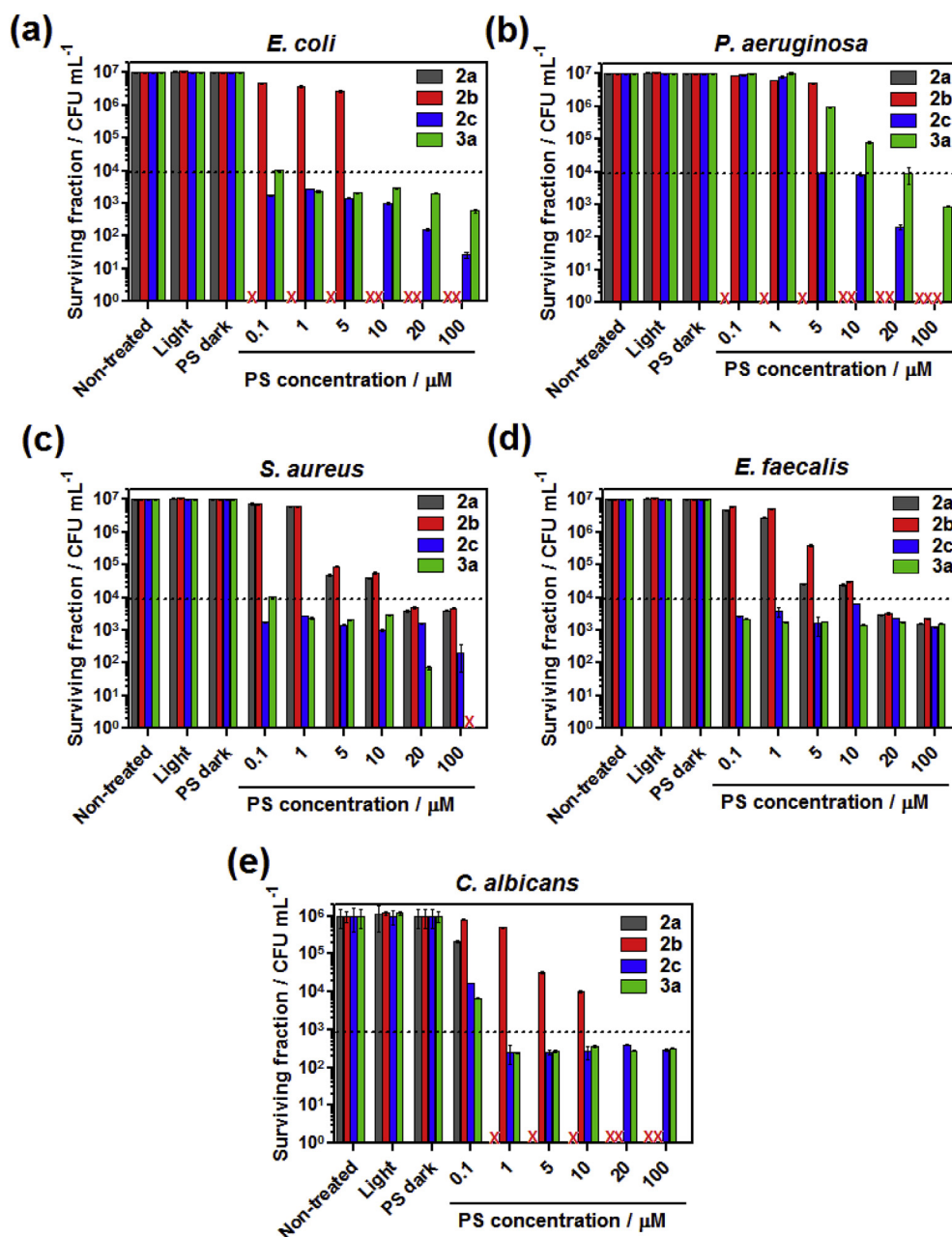


Fig. 5. Photoinactivation of bacteria and fungi irradiated with a light dose of 10 J/cm^2 : (a) *E. coli*, (b) *P. aeruginosa*, (c) *S. aureus*, (d) *E. faecalis*, (e) *C. albicans*.

Table 4

MIC values of investigated phthalocyanines determined for a light dose of 10 J/cm^2 .

Microorganism	MIC [$\mu\text{g/mL}$]			
	2a	2b	2c	3a
<i>E. coli</i>	0.13	15	nd	nd
<i>P. aeruginosa</i>	0.13	15	218	nd
<i>S. aureus</i>	nd	nd	nd	106
<i>C. albicans</i>	1.4	31	nd	nd

nd – not determined.

photosensitizers. The influence of these photosensitizer populations on PDI efficacy was tested in a protocol including a washing step to remove the unbound photosensitizer fraction. A marked decrease in the inactivation of all types of microbial cells

was observed for both **2a** and **2b** (Fig. 6). The photosensitizer does not need to be internalized by the bacteria to contribute to PDI, which explains the lack of correlation between uptake and PDI efficacy. In topical applications, which are the most likely to be translated to the clinic because PDI is a local treatment, it is unlikely that the treatment protocol needs to include a washing step after the application of the topical formulation.

Intracellular imaging with CLSM. The microenvironment may alter the fluorescence intensity signal with the uptake of the photosensitizer [68]. Therefore, to confirm the intracellular accumulation of phthalocyanines in Gram-positive bacteria (*S. aureus*), Gram-negative bacteria (*E. coli*) and fungal yeast (*C. albicans*), we performed confocal laser scanning microscopy (CLSM). Fig. 7a–c presents the images obtained for **2b**, which exhibits the highest accumulation in these microorganisms. All microorganisms became

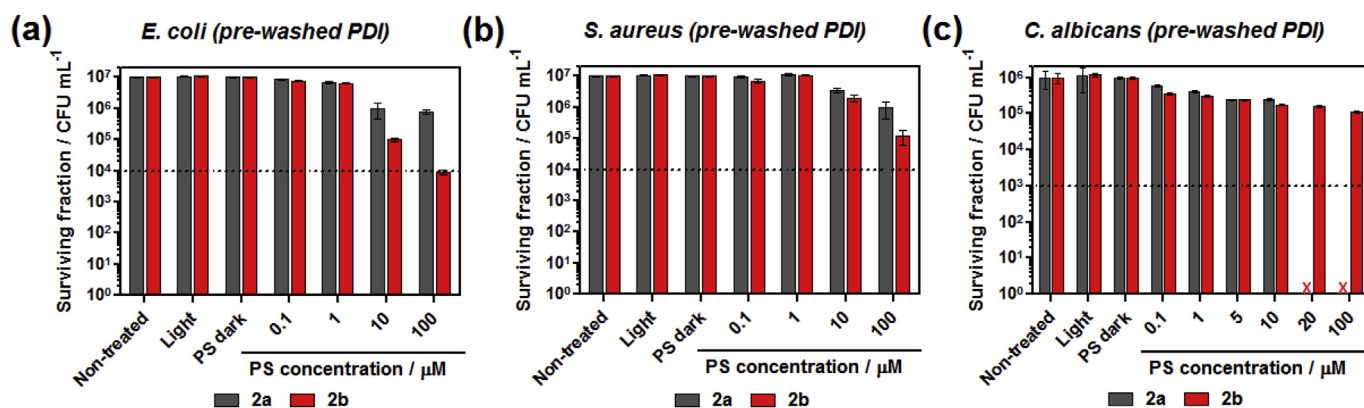


Fig. 6. Photoinactivation of (a) *E. coli*, (b) *S. aureus* and (c) *C. albicans* with 2a and 2b phthalocyanines washed with PBS before irradiation. In all experiments a light dose of 10 J/cm² was used.

highly fluorescent after incubation with phthalocyanines, which proves that these photosensitizers are not aggregated in the cells. This can be best appreciated by inspection of the fluorescence emission profile along a cross section of a cell, as reported in Fig. 7d. Similar results were obtained for the other phthalocyanines (Figure 14, Data in Brief). The uptake by *C. albicans* (Fig. 7c) is at similar level as those obtained *E. coli* and *S. aureus*, which is consistent with Fig. 4. Confocal microscopy also enables spatially well-defined measurements inside the cells (z-stack, Fig. 7d), which confirm the presence of 2b inside the bacterial cells. It is worth to highlight that these results were achieved without the addition of membrane disruptors, which may be added to improve uptake [8,11].

Dark cytotoxicity and photocytotoxicity against eukaryotic cells. The viability of immortalized HaCaT (human keratinocyte) cells was not significantly affected by phthalocyanine concentrations below 10 μM in the dark. Toxicity (~50% reduction in survival) was only observed at the highest tested concentration of 100 μM (Fig. 8a). Hence, these phthalocyanines have low cytotoxicity against eukaryotic cells in the dark. When the phototoxicity of cationic phthalocyanines against eukaryotic cells was evaluated using the same PDT protocol as that used through this study to assess PDI of bacteria and fungi, neither of tested compounds showed significant toxicity at 0.1 μM as determined in cell survival MTT assay (Fig. 8b). The phototoxicity of all phthalocyanines increased with concentration until ca. 10 μM , where it reached a plateau of cellular viability. In the 0.1–5 μM concentration range, 3a was the least cytotoxic, while 2c was more toxic to cells, particularly at higher concentrations. Longer incubation times, more typical of photodynamic therapy of cancer at long drug-to-light intervals, led to slightly increased phototoxicity. This is related with increased cellular uptake by HaCaT cells at longer incubation times (from 2 h to 24 h).

3. Conclusion

A new family of tetra-imidazolyl substituted metallophthalocyanines was synthesized in high yields to evaluate structure-activity relationships in PDI of bacteria and fungi. Three structural motifs were investigated: size of cationizing alkyl chain, degree of cationization and central diamagnetic metal. Cationic Zn(II) metallophthalocyanines were found to have high molar absorption coefficients ($2.4 < \epsilon < 2.8$ in units of $10^5 \text{ M}^{-1} \text{ cm}^{-1}$) and high singlet oxygen quantum yields ($0.66 < \Phi_{\Delta} < 0.72$). Zn(II) tetra-ethyl cationic phthalocyanine 2a showed the highest PDI efficacy against Gram-negative bacteria and *C. albicans*, with a 6 logs reduction of their viability at photosensitizer concentrations as low

as 100 nM and 1 μM , respectively. These cationic photosensitizers have low toxicity towards human keratinocytes (HaCaT cell line) at concentrations effective in killing Gram-negative bacteria. The selectivity of cationic phthalocyanines towards inactivation of Gram-negative bacteria rather than for PDT of eukaryotic cells was already noted by other authors [43,75], and is possibly related to the higher number of anionic biomolecules present at the surface of Gram-negative bacteria. The photosensitizers do not need to be internalized by the bacteria to photoinactivate them, at least when singlet oxygen is the predominant ROS.

A larger number of positive charges in the photosensitizer (8 vs. 4) does not necessarily improve PDI of Gram-negative bacteria. The higher water solubility acquired with many charges may diminish the interaction with bacteria. A higher lipophilicity will improve uptake but not necessarily impact on efficacy, especially when PDI is performed without previously washing the cells to remove unbound or electrostatically attached photosensitizer molecules. The success with Zn(II) tetra-ethyl cationic phthalocyanine 2a results from a moderate number of positive charges, a short alkyl chain, a metal cation that favours intersystem crossing to the triplet state and no low-lying charge-transfer states, and high singlet oxygen quantum yield. Photosensitizer 2a is a good lead to PDI of topical infections.

4. Experimental section

Materials and equipment. All solvents were dried according to standard procedures. Commercial reagents were from Sigma-Aldrich and Fluorochem and were used without further purification. UV–vis spectra were recorded on Hitachi U-2001 or Shimadzu 2100 spectrophotometers. Nuclear magnetic resonance ¹H and ¹³C spectra were recorded on 400 Bruker Avance spectrometer (400 and 101 MHz, respectively), using tetramethylsilane ($\delta = 0.00$ ppm) as internal standard. The EI and ESI mass spectra were acquired using a Autospec Micromass and Bruker Microtof, respectively. Fluorescence spectra were obtained in a Horiba Jobin Yvon – Spex Fluorolog 3.22. For determination of singlet oxygen quantum yields excitation with the third harmonics of a Spectra-Physics Quanta-Ray GCR-130 Nd–YAG laser was used. Singlet oxygen phosphorescence was collected at 1270 nm using a Hamamatsu R5509-42 photomultiplier cooled to 193 K in a liquid nitrogen chamber [76].

5. Synthesis

5.1. 4-(1'H-imidazol-1'-yl)phthalonitrile (1)

Imidazole (1.26 g, 18.5 mmol) was added to a solution of 4-

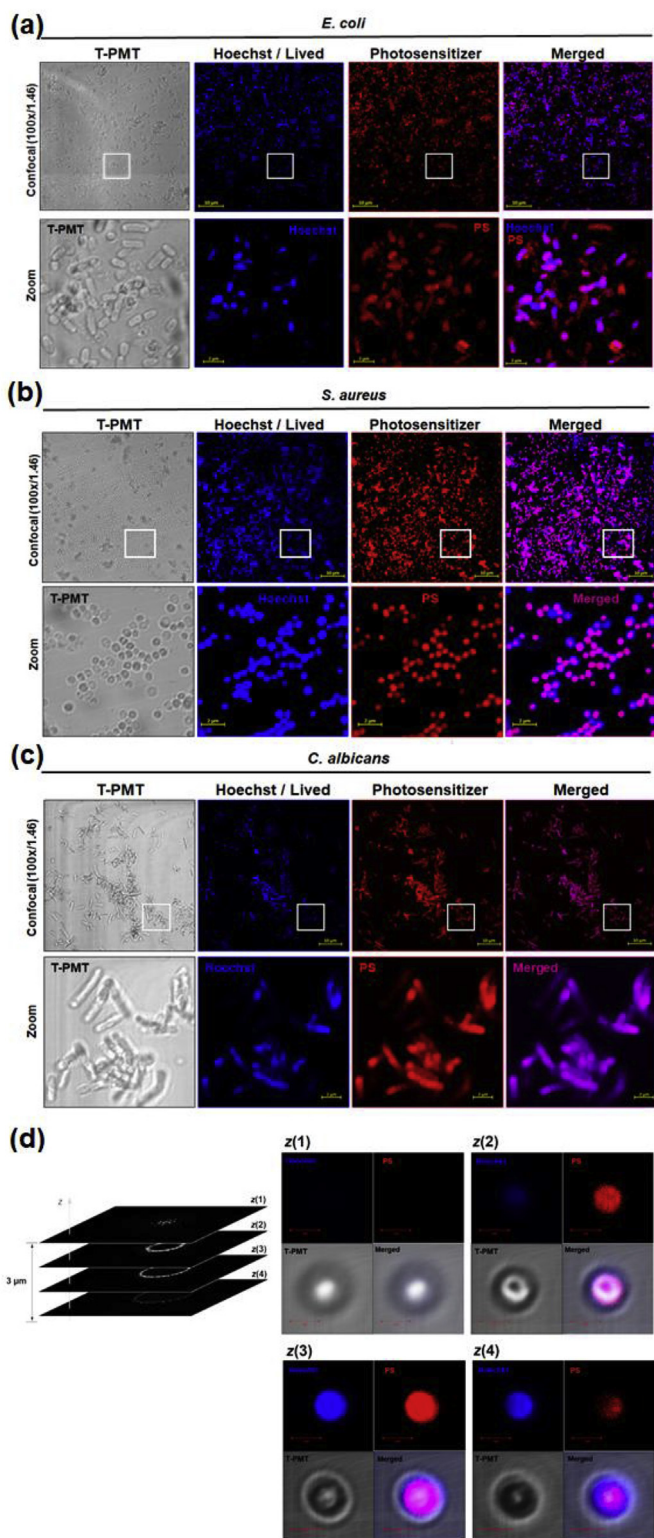


Fig. 7. Confocal laser scanning microscopy images of (a) *E. coli*, (b) *S. aureus*, (c) *C. albicans* after incubation with 10 μ M of cationic phthalocyanine **2b** showing transmitted light differential interference contrast images, living bacteria stained with Hoechst, accumulation of PS in bacteria (red fluorescence), merged images that show localization of photosensitizer and the images registered at higher zoom (bottom panels); (d) Sectioning (Z-stack) images at different focal planes that visualize the intracellular accumulation of PS in bacteria cells. (For interpretation of the references to colour in this figure legend, the reader is referred to the Web version of this article.)

nitrophthlonitrile (2.56 g, 14.8 mmol) and K_2CO_3 (10.2 g, 74 mmol) in DMF (38 ml). The reaction mixture was left at room temperature for 48 h. The base was filtered and the filtrate was washed with a small amount of DMF. The reaction mixture was added to a mixture of water and ice (200 ml) and the yellow precipitate was filtered. To the precipitate, methanol (50 ml) was added and the mixture was heated with vigorous stirring. After cooling, the light-yellow precipitate was filtered. Yield: 1.59 g (56%). 1H NMR (400 MHz, $DMSO-d_6$): δ = 8.58 (d, J = 1.7 Hz, 1H, H3); 8.53 (s, 1H, H2'); 8.29–8.22 (m, 2H, H5+H6); 7.98 (s, 1H, H5'); 7.18 (s, 1H, H4'). ^{13}C NMR (101 MHz, $DMSO-d_6$): δ = 140.23 (C4); 136.00 (C2'); 135.70 (C6); 130.92 (C4'); 124.44 (C3); 124.02 (C5); 117.60 (C5'); 116.44 (C1); 115.61 (C1–CN); 115.39 (C2–CN); 111.67 (C2). MS (EI): Calc. 194.0592; Found: 194.0591 $[M]^+$.

5.2. 2(3),9(10),16(17),23(24)-tetrakis(1'-H-imidazol-1'-yl)phthalocyanato zinc (II) (2)

A mixture of 4-(1'-H-imidazol-1'-yl)phthalonitrile (**1**) (502 mg, 2.58 mmol) and $Zn(OAc)_2 \cdot 2H_2O$ (284 mg, 1.29 mmol) was refluxed in DMAE (4 ml) for 48 h in inert atmosphere. After cooling, the product was precipitated by addition of a mixture of methanol and water and filtered. The green precipitate was washed with 25 ml of water, methanol, acetone and dichloromethane. Yield: 385 mg (71%). UV–Vis ($DMSO$): λ , nm ($\log \epsilon$, $M^{-1} cm^{-1}$): 358 (4.40); 616 (4.11); 682 (4.85). 1H NMR (400 MHz, Pyridine- d_5 , 80 °C): δ = 9.41–9.24 (m, 8H); 8.91–8.83 (m, 4H); 8.31–8.06 (m, 8H); 7.76 (d, J = 10.3 Hz, 4H). MS (ESI-TOF): Calc. 841.1740 Found: 841.1735 $[M+H]^+$.

5.3. 2(3),9(10),16(17),23(24)-tetrakis(3'-ethyl-1'-H-imidazol-1'-yl)phthalocyanato zinc (II) iodide (2a)

Phthalocyanine **2** (100 mg, 0.119 mmol) and iodoethane (1 ml, 12 mmol) were dissolved in DMF (4 ml). The reaction proceeded at 75 °C for 48 h in inert atmosphere and an additional 3 ml (36 mmol) of iodoethane was added during this period. The product was precipitated with the addition of 40 ml DCM and filtered. Yield: 85 mg (49%). UV–Vis ($DMSO$): λ , nm ($\log \epsilon$, $M^{-1} cm^{-1}$): 354 (4.87); 611 (4.64); 677 (5.45). 1H NMR (400 MHz, $DMSO-d_6$): δ = 10.50–10.10 (m, 4H); 9.80–9.05 (m, 4H); 9.00–8.50 (m, 8H); 8.44–8.08 (m, 8H); 4.45 (br, 8H); 1.62 (br, 12H). MS (ESI-TOF): Calc. 1337.0344 Found: 1337.0397 $[M-I]^+$.

5.4. 2(3),9(10),16(17),23(24)-tetrakis(3'-octyl-1'-H-imidazol-1'-yl)phthalocyanato zinc (II) iodide (2b)

Phthalocyanine **2** (150 mg, 0.18 mmol) and iodoctane (0.3 ml, 1.8 mmol) were dissolved in DMF (5 ml). The reaction proceeded at 100 °C for 48 h in inert atmosphere and an additional 0.3 ml (1.8 mmol) of iodoctane were added during this period. After cooling, 20 ml of methanol were added and the product was precipitated by 150 ml of Et_2O . Yield: 128 mg (40%). UV–Vis ($DMSO$): λ , nm ($\log \epsilon$, $M^{-1} cm^{-1}$): 354 (4.79); 611 (4.57); 677 (5.38). 1H NMR (400 MHz, $DMSO-d_6$): δ = 10.90–10.00 (m, 4H); 9.90–8.75 (m, 10H); 8.67–8.00 (m, 10H); 4.65–4.15 (m, 8H); 2.30–2.20 (m, 8H); 1.60–1.11 (m, 40H); 0.95–0.75 (m, 12H). MS (ESI-TOF): Calc. 1546.5050 Found: 1546.5058 $[M-2I]^+$.

5.5. 2(3),9(10),16(17),23(24)-tetrakis(3'-(2''-ethyltrimethylammonium)-1'-H-imidazol-1'-yl)phthalocyanato zinc (II) iodide (2c)

Phthalocyanine **2** (166 mg, 0.20 mmol), (2-chloroethyl)trimethylammonium chloride (322 mg, 2.10 mmol) and KI (3.5 g,

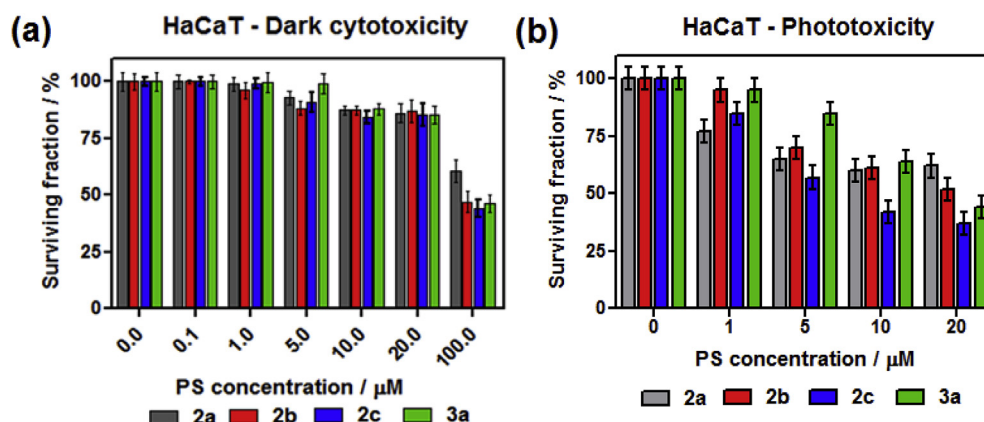


Fig. 8. Cytotoxicity of **2a-2c** and **3a** phthalocyanines against human keratinocyte (HaCaT) cells. (a) Dark cytotoxicity. (b) Photocytotoxicity determined for various concentrations after irradiation with white light at 10 J/cm^2 under the conditions of PDI of bacteria.

21.0 mmol) were mixed in DMF (5 ml). The reaction proceeded at 120°C for 72 h in inert atmosphere. After cooling, dichloromethane (30 ml) was added. The precipitate was washed with ethanol ($4 \times 20\text{ ml}$) using ultrasounds and filtered. The resulting solid was dissolved in H_2O and was subjected to a size exclusion chromatography using Sephadex® G-10 with a flow rate of 2.5 ml/min . Yield: 125 mg (42%). UV–Vis (DMSO): λ , nm ($\log \epsilon$, $\text{M}^{-1}\text{cm}^{-1}$): 343 (4.74); 612 (4.56); 677 (5.41). ^1H NMR (400 MHz, $\text{DMSO}-d_6$): δ = 10.78 (br, 2H); 10.40 (br, 2H); 10.00–9.25 (br, 8H); 8.96–8.20 (m, 16H); 5.16 (br, 4H); 4.17 (m, 12H). Anal. Calcd. for $\text{C}_{64}\text{H}_{76}\text{I}_8\text{N}_{20}\text{Zn}_4$ KI: C 26.79; H 2.64; N 9.76%. Found: C 26.88; H 2.64; N 9.76%.

5.6. 2(3),9(10),16(17),23(24)-tetrakis(1'-H-imidazol-1'-yl)phthalocyanato hydroxyaluminium (III) (**3**)

A mixture of 4-(1'-H-imidazol-1'-yl)phthalonitrile (**1**) (500 mg, 2.57 mmol) and AlCl_3 (171 mg, 1.28 mmol) was heated to 240°C in 1-chloronaphthalene (5 ml) for 7 h, under inert atmosphere. After cooling, the product was precipitated by addition of dichloromethane and filtered-off. The green precipitate was washed with 25 ml of acetone, water, acetone and finally dichloromethane. Yield: 340 mg (60%). UV–Vis (DMSO): λ , nm ($\log \epsilon$, $\text{M}^{-1}\text{cm}^{-1}$): 364 (4.85); 624 (4.54); 693 (5.26). ^1H NMR (400 MHz, $\text{DMSO}-d_6$): δ = 10.00 (s, 4H); 9.82 (m, 4H); 9.29 (m, 4H); 8.88 (m, 4H); 8.55 (m, 4H); 7.60 (s, 4H). MS (ESI-TOF): Calc. 821,2291 Found: 821,2285 $[\text{M}+\text{H}]^+$.

5.7. 2(3),9(10),16(17),23(24)-tetrakis(3'-ethyl-1'-H-imidazol-1'-yl)phthalocyanato hydroxyaluminium (III) iodide (**3a**)

Phthalocyanine **3** (120 mg, 0.14 mmol) and iodoethane (1 ml, 12 mmol) were dissolved in DMF (4 ml). The reaction proceeded at 75°C for 48 h under inert atmosphere and an additional 3 ml (36 mmol) of iodoethane were added during this period. The product was precipitated with the addition of 20 ml DCM and filtered. Yield: 155 mg (79%). UV–Vis (DMSO): λ , nm ($\log \epsilon$, $\text{M}^{-1}\text{cm}^{-1}$): 357 (4.85); 616 (4.48); 680 (5.23). ^1H NMR (400 MHz, $\text{DMSO}-d_6$): δ = 10.55 (m, 4H); 10.33–10.21 (m, 4H); 9.99 (m, 4H); 8.98 (m, 8H); 8.37 (s, 4H); 4.54 (q, $J = 7.3\text{ Hz}$, 8H); 1.73 (t, $J = 7.3\text{ Hz}$, 12H). MS (ESI-TOF): Calc. 1061.2660 Found: 1061.2698 $[\text{M}-3\text{I}-2\text{H}]^+$.

Molar absorption coefficients. Molar absorption coefficients were determined according to Beer-Lambert's law. For each compound, a minimum of 6 solutions were prepared in concentrations ranging from 10^{-7} to 10^{-6} M corresponding to absorbance values between 0.1 and 1.2.

Fluorescence quantum yield. Fluorescence quantum yields (Φ_F) were determined in DMSO using a comparative method, according to equation (1):

$$\Phi_F = \Phi_F^{\text{Std}} \frac{F A_{\text{Std}} \eta^2}{F_{\text{Std}} A \eta_{\text{Std}}^2} \quad (1)$$

where F and F_{Std} are the integrals of the fluorescence emission curves of the samples and the standard, respectively; A and A_{Std} are the respective absorbances of the samples and standard at the excitation wavelengths, respectively; η^2 and η_{Std}^2 are the refractive indices of solvents used for the sample and standard, respectively. Unsubstituted Zinc(II) phthalocyanine (ZnPc) in DMSO ($\Phi_F = 0.18$)⁶⁴ was used as a standard. The absorbance of tested solutions at the excitation wavelength (610–630 nm) ranged between 0.03 and 0.05, which corresponded to concentrations in the range of $1.0\text{--}3.0 \cdot 10^{-6}\text{ M}$.

Singlet oxygen quantum yield. Singlet oxygen quantum yields (Φ_Δ) were determined in DMSO using a comparative method and direct measurement of singlet oxygen phosphorescence at 1270 nm. Decay curves of the singlet molecular oxygen emission were extrapolated to time-zero for the reference (ZnPc, $\Phi_\Delta^{\text{Std}} = 0.67$)⁶⁴ and for the samples to obtain a relation between emission intensities at a given laser power. This relation is identical to the relation between the singlet molecular oxygen quantum yields. The actual singlet oxygen quantum yields were obtained by comparing the linear dependence between and the energy of the laser pulse for the sample (S) and the reference (S_{Std}) using (2):

$$\Phi_\Delta = \Phi_\Delta^{\text{Std}} \frac{S}{1 - 10^{-A}} \cdot \frac{1 - 10^{-A_{\text{Std}}}}{S_{\text{Std}}} \quad (2)$$

where A and A_{Std} are the absorbance of the sample and the reference, respectively.

Detection of reactive oxygen species in solution. 3'-*p*-(aminophenyl)fluorescein (APF) and 3'-*p*-(hydroxyphenyl)fluorescein (HPF) were used to detect hydroxyl radicals. Singlet Oxygen Sensor Green® (SOSG) was used to probe for singlet oxygen. Dihydroethidium (DHE) was used to identify the superoxide ion. The probes were employed for the detection of ROS after illumination of the photosensitizer. PS solutions were diluted to a final concentration of $10\text{ }\mu\text{M}$ per well. Tested fluorescent probes were added at a final concentration of $15\text{ }\mu\text{M}$. Photosensitizer's solutions were irradiated with white light using a 150 W fiber optical illuminator (OSH150) light for various time intervals. A microplate reader

(Tecan Infinite M200 Reader) was used for acquisition of fluorescence signal immediately before and after illumination. For APF fluorescence emission at 515 nm was determined upon excitation at 490 nm. For SOSG, the corresponding values were 525 and 505 nm, and 480 nm and 580 nm for DHE.

Log P_{ow} determination. The *n*-octanol/PBS partition coefficients (logP) were measured following shake-flask method with minor modifications as describe before. The photosensitizers were dissolved in the mixture of *n*-octanol previously saturated with a solution of PBS and the same volume of PBS saturated with *n*-octanol. After addition of the samples of each phthalocyanine the solutions were mixed on a vortex device and then the phases were separated by centrifugation (15 min, 8000 rpm, RT). Next, the PBS/*n*-octanol phase was taken and diluted to obtain 0.5% of PBS/*n*-octanol content in the final solution. This solution was left into the ultrasonic bath. The fluorescence of each solution was measured using Fluorescence Spectrometer LS 55 (PerkinElmer) and compared with calibration curve to obtain the concentration of the photosensitizer. Partition coefficients were calculated from the ratio C_{oct}/C_{PBS} , where C_{oct} and C_{PBS} are the concentrations of the porphyrin derivatives in the *n*-octanol and in the PBS.

Binding of photosensitizer to microorganisms – uptake studies. The microorganisms were incubated in suspension with phthalocyanines (10 μ M) for selected intervals (10–120 min) in the dark at RT. Unbound photosensitizer was removed by washing twice in PBS without Ca^{2+} and Mg^{2+} . After the second wash the cells were lysed in 10% SDS for 24 h. The cellular uptake of the photosensitizer was evaluated by determination of fluorescence using excitation at Soret band (ca. 340–360 nm) and emission between 600 and 750 nm (Tecan Infinite M200 Reader). Calibration curves were prepared in 10% SDS and used for determination of PS concentration. Uptake values were obtained by dividing the PS concentration by the number of CFU. The number of molecules per cell was calculated from concentration.

Photoinactivation of microorganisms. Both Gram-positive bacteria (*S. aureus*, *E. faecalis*) and Gram-negative bacteria (*E. coli* and *P. aeruginosa*) were used in this study. *E. coli*, *P. aeruginosa* and *E. faecalis* were cultured in LB Broth/Lennox (BioShop Lab Science Products), while *S. aureus* was grown in Brain Heart Infusion (BHI) broth (Sigma Aldrich) in an orbital incubator (37 °C, 130 rpm), until the absorbance reached 0.5, which corresponded to approximately 10^7 CFU per mL. *C. albicans* were cultured overnight in YPD Broth (BioShop) with aeration at 30 °C reaching ca. 10^6 CFU/mL. Tested microorganisms were incubated with various concentrations of the phthalocyanines at pH 7.4 (PBS) for 1–2 h in the dark at room temperature. Aliquots (1 mL) were transferred to a 12-well plate and illuminated with white light (using a 150 W fiber optical illuminator (OSH150)). After illumination (or dark incubation - control) samples were mixed, serial-diluted in PBS and plated (LB agar) to determine the number of CFU. Cells treated only with light (no photosensitizer) were as viable as untreated cells (data not shown). The viability was also monitored using LIVE/DEAD BacLight Bacterial Viability Kit (Invitrogen; monitors membrane integrity) according to manufacturer's instructions.

Laser scanning confocal microscopy (LSCM) imaging. The accumulation of cationic phthalocyanines in microorganisms was followed with confocal imaging using a Zeiss LSM880 laser-scanning microscope equipped with an argon ion laser. The objective used was a water immersion 'dipping' lens (63x, Carl Zeiss Ltd.) with a working distance of 1.46 mm. Selected bacteria or fungi cells were incubated with the phthalocyanine for an appropriate time interval determined in uptake studies. After washing, the microorganism cells were placed on the microscopic glass slides and imaged. The separation between focal planes in Z-stack images was 0.25 μ m. Registered images were analysed with the Zeiss ZEN

software.

Mammalian cell-based assays. Human keratinocytes (HaCaT) were cultured in DMEM (BioTech) with addition of 10% foetal bovine serum (BioTech, Poland) and supplemented with 1% antibiotics (penicillin/streptomycin). For experiments the cells were removed by trypsinization, washed with PBS and maintained in a humidified atmosphere at 37 °C and 5% CO₂.

Cytotoxicity in the dark. HaCaT cells were seeded in 96 well plates (10^4 per well) and after attachment photosensitizer was added in Hanks Balanced Salt Saline (DMSO<0.5%) at concentrations between 0 and 100 μ M. Cells were incubated for 2 h or 24 h at 37 °C in the dark. Photosensitizer was removed, cells were washed in PBS with Ca^{2+} and Mg^{2+} and 200 μ l fresh culture medium supplemented with FBS and antibiotics was added to each well. After 24 h cell viability was determined by MTT assay. Briefly, MTT was dissolved at 5 mg/ml in PBS and added to each well at 0.5 mg/ml. After 3–4 h incubation the medium was discarded and 100 μ l of DMSO/methanol (1:1) was added to dissolve the dark blue crystals of formazan. Formazan quantification was performed using an automatic microplate reader (Tecan Infinite M200 Reader) by absorbance measurements at 565 nm. Experiments were performed in triplicates. Data are expressed as mean absorbance value of six samples obtained in each independent experiments and standard error of the mean.

Photodynamic effect. The cells were incubated in the dark with photosensitizer (0.1–100 μ M) in HBSS for 2 h or 24 h and irradiated with 10 J/cm² white light using a 150 W fiber optical illuminator (OSH150). Following irradiation, the cells were washed with fresh medium and plates were returned to the incubator. Cell viability was determined by MTT viability assay (see above) 24 h after irradiation.

Statistics. All values are expressed as average \pm SEM (standard error of the mean), which represents the standard deviation of the sample mean estimate of a population mean. All experiments were repeated at least three times with comparable results. The sample size in biological tests was $N = 6$ –12 in each experimental group. Experiments were also repeated at least three times with comparable results. The *t*-test was used for the determination of statistical significance. Results were considered as statistically significant with a confidence level of 95% ($p < 0.05$). Statistical analysis was performed with the STATISTICA 12.5 (StatSoft Poland, Krakow).

Acknowledgements

We thank Fundação para a Ciência e a Tecnologia (FCT), Portugal (grants UID/QUI/00313/2019, PTDC/QEQ-MED/3521/2014 and POCI-01-0145-FEDER-027996), and the National Science Center (NCN), Poland (Sonata Bis grant number 2016/22/E/NZ7/00420 given to JMD). RTA thanks FCT for the scholarship PD/BI/135341/2017, and BP thanks the Foundation for Polish Science for START 071.2019 programme. Some of the research was carried out with equipment purchased with the financial support of the European Regional Development Fund in the framework of the Polish Innovation Economy Operational Program (contract no. POIG.02.01.00-12-167/08).

Appendix A. Supplementary data

Supplementary data to this article can be found online at <https://doi.org/10.1016/j.ejmech.2019.111740>.

References

- [1] W.H. Organization, Global Antimicrobial Resistance Surveillance System (GLASS) Report: Early Implementation 2017–2018, 2018.

- [2] J. O'Neill, et al., Antimicrobial resistance: Tackling a crisis for the health and wealth of nations, *Rev. Antimicrob. Resist.* (2014) 1–20.
- [3] S. Shrivastava, P. Shrivastava, J. Ramasamy, World health organization releases global priority list of antibiotic-resistant bacteria to guide research, discovery, and development of new antibiotics, *J. Med. Soc.* 32 (1) (2018), 76–76.
- [4] M.S. Butler, M.A. Blaskovich, M.A. Cooper, Antibiotics in the clinical pipeline at the end of 2015, *J. Antibiot.* 70 (1) (2017) 3.
- [5] T.J. Silhavy, D. Kahne, S. Walker, The bacterial cell envelope, *Cold Spring Harb. Perspect. Biol.* 2 (5) (2010) a000414.
- [6] K. Lewis, Platforms for antibiotic discovery, *Nat. Rev. Drug Discov.* 12 (5) (2013) 371.
- [7] A. Regiel-Futyr, J.M. Dąbrowski, O. Mazuryk, K. Śpiwak, A. Kyzioł, B. Pucelik, M. Brindell, G. Stochel, Bioinorganic antimicrobial strategies in the resistance era, *Coord. Chem. Rev.* 351 (2017) 76–117.
- [8] M.R. Hamblin, G. Jori, Photodynamic Inactivation of Microbial Pathogens: Medical and Environmental Application, The Royal Society of Chemistry, Cambridge, 2011.
- [9] H. Mahmoudi, A. Bahador, M. Pourhajibagher, M.Y. Alikhani, Antimicrobial photodynamic therapy: an effective alternative approach to control bacterial infections, *J. Laser Med. Sci.* 9 (3) (2018) 154.
- [10] V.S. Ghatge, W. Zhou, H.G. Yuk, Perspectives and trends in the application of photodynamic inactivation for microbiological food safety, *Compr. Rev. Food Sci. Food Saf.* 18 (2) (2019) 402–424.
- [11] M. Wainwright, T. Maisch, S. Nonell, K. Plaetzer, A. Almeida, G.P. Tegos, M.R. Hamblin, Photoantimicrobials—are we afraid of the light? *Lancet Infect. Dis.* 17 (2) (2017) e49–e55.
- [12] M.R. Hamblin, T. Hasan, Photodynamic therapy: a new antimicrobial approach to infectious disease? *Photochem. Photobiol. Sci.* 3 (5) (2004) 436–450.
- [13] J. Almeida, J.P. Tomé, M.G. Neves, A.C. Tomé, J.A. Cavaleiro, A. Cunha, L. Costa, M.A. Faustino, A. Almeida, Photodynamic inactivation of multidrug-resistant bacteria in hospital wastewaters: influence of residual antibiotics, *Photochem. Photobiol. Sci.* 13 (4) (2014) 626–633.
- [14] T. Maisch, A. Eichner, A. Späth, A. Gollmer, B. König, J. Regensburger, W. Bäuml, Fast and effective photodynamic inactivation of multi-resistant bacteria by cationic riboflavin derivatives, *PLoS One* 9 (12) (2014) e111792.
- [15] P. Agostinis, K. Berg, K.A. Cengel, T.H. Foster, A.W. Girotti, S.O. Gollnick, S.M. Hahn, M.R. Hamblin, A. Juzeniene, D. Kessel, M. Korbelik, J. Moan, P. Mroz, D. Nowis, J. Piette, B.C. Wilson, J. Golab, Photodynamic therapy of cancer: an update, *CA A Cancer J. Clin.* 61 (4) (2011) 250–281.
- [16] J.M. Dąbrowski, Reactive oxygen species in photodynamic therapy: mechanisms of their generation and potentiation, in: *Advances in Inorganic Chemistry*, vol. 70, Elsevier, 2017, pp. 343–394.
- [17] M. Oszejka, M. Brindell, Ł. Orzel, J.M. Dąbrowski, K. Śpiwak, P. Łabuz, M. Pacia, A. Stochel-Gaudyn, W. Macyk, R. van Eldik, Mechanistic studies on versatile metal-assisted hydrogen peroxide activation processes for biomedical and environmental incentives, *Coord. Chem. Rev.* 327 (2016) 143–165.
- [18] A. Sutek, B. Pucelik, J. Kunciewicz, G. Dubin, J.M. Dąbrowski, Sensitization of TiO₂ by halogenated porphyrin derivatives for visible light biomedical and environmental photocatalysis, *Catal. Today* 335 (2019) 538–549.
- [19] S. Hatz, J.D. Lambert, P.R. Ogilby, Measuring the lifetime of singlet oxygen in a single cell: addressing the issue of cell viability, *Photochem. Photobiol. Sci.* 6 (10) (2007) 1106–1116.
- [20] T. Maisch, Resistance in antimicrobial photodynamic inactivation of bacteria, *Photochem. Photobiol. Sci.* 14 (8) (2015) 1518–1526.
- [21] T.G. St Denis, T. Dai, L. Izikson, C. Astrakas, R.R. Anderson, M.R. Hamblin, G.P. Tegos, All you need is light: antimicrobial photoinactivation as an evolving and emerging discovery strategy against infectious disease, *Virulence* 2 (6) (2011) 509–520.
- [22] A. Kawczyk-Krupka, B. Pucelik, A. Międzybrodzka, A. Sieroń, J.M. Dąbrowski, Photodynamic therapy as an alternative to antibiotic therapy for the treatment of infected leg ulcers, *Photodiagn. Photodyn. Ther.* 23 (2018) 132–143.
- [23] J. Staroń, J.M. Dąbrowski, E. Cichoń, M. Guzik, Lactose esters: synthesis and biotechnological applications, *Crit. Rev. Biotechnol.* 38 (2) (2018) 245–258.
- [24] N. Kömerik, M. Wilson, S. Poole, The effect of photodynamic action on two virulence factors of gram-negative bacteria, *Photochem. Photobiol.* 72 (5) (2000) 676–680.
- [25] F. Sperandio, Y.-Y. Huang, M. R. Hamblin, Antimicrobial photodynamic therapy to kill Gram-negative bacteria, *Recent Pat. Anti-Infect. Drug Discov.* 8 (2) (2013) 108–120.
- [26] T. Maisch, A new strategy to destroy antibiotic resistant microorganisms: antimicrobial photodynamic treatment, *Mini Rev. Med. Chem.* 9 (8) (2009) 974–983.
- [27] B. Pucelik, I. Gürol, V. Ahsen, F. Dumoulin, J.M. Dąbrowski, Fluorination of phthalocyanine substituents: improved photophysical properties and enhanced photodynamic efficacy after optimal micellar formulations, *Eur. J. Med. Chem.* 124 (2016) 284–298.
- [28] J.M. Dąbrowski, B. Pucelik, A. Regiel-Futyr, M. Brindell, O. Mazuryk, A. Kyzioł, G. Stochel, W. Macyk, L.G. Arnaut, Engineering of relevant photodynamic processes through structural modifications of metallotetrapyrrolic photosensitizers, *Coord. Chem. Rev.* 325 (2016) 67–101.
- [29] S.Z. Topal, Ü. İsci, U. Kumru, D. Atilla, A.G. Gürek, C. Hırel, M. Durmuş, J.-B. Tommasino, D. Luneau, S. Berber, Modulation of the electronic and spectroscopic properties of Zn (II) phthalocyanines by their substitution pattern, *Dalton Trans.* 43 (18) (2014) 6897–6908.
- [30] A. Minnock, D.I. Vernon, J. Schofield, J. Griffiths, J.H. Parish, S.B. Brown, Photoinactivation of bacteria. Use of a cationic water-soluble zinc phthalocyanine to photoinactivate both gram-negative and gram-positive bacteria, *J. Photochem. Photobiol. B Biol.* 32 (3) (1996) 159–164.
- [31] M. Merchat, G. Bertolini, P. Giacomini, A. Villaneuva, G. Jori, Meso-substituted cationic porphyrins as efficient photosensitizers of gram-positive and gram-negative bacteria, *J. Photochem. Photobiol. B Biol.* 32 (3) (1996) 153–157.
- [32] G.P. Tegos, M. Anbe, C. Yang, T.N. Demidova, M. Satti, P. Mroz, S. Janjua, F. Gad, M.R. Hamblin, Protease-stable polycationic photosensitizer conjugates between polyethyleneimine and chlorin (e6) for broad-spectrum antimicrobial photoinactivation, *Antimicrob. Agents Chemother.* 50 (4) (2006) 1402–1410.
- [33] K. Winkler, C. Simon, M. Finke, K. Bleses, M. Birke, N. Szentmáry, D. Hüttenberger, T. Eppig, T. Stachon, A. Langenbucher, Photodynamic inactivation of multidrug-resistant *Staphylococcus aureus* by chlorin e6 and red light ($\lambda = 670$ nm), *J. Photochem. Photobiol. B Biol.* 162 (2016) 340–347.
- [34] L. Huang, Y.-Y. Huang, P. Mroz, G.P. Tegos, T. Zhiyentayev, S.K. Sharma, Z. Lu, T. Balasubramanian, M. Krayer, C. Ruzié, Stable synthetic cationic bacteriochlorins as selective antimicrobial photosensitizers, *Antimicrob. Agents Chemother.* 54 (9) (2010) 3834–3841.
- [35] L. Huang, M. Krayer, J.G.S. Roubil, Y.Y. Huang, D. Holten, J.S. Lindsey, M.R. Hamblin, Stable synthetic mono-substituted cationic bacteriochlorins mediate selective broad-spectrum photoinactivation of drug-resistant pathogens at nanomolar concentrations, *J. Photochem. Photobiol., B* 141 (2014) 119–127.
- [36] X. Ragas, D. Sánchez-García, R. Ruiz-González, T. Dai, M. Agut, M.R. Hamblin, S. Nonell, Cationic porphyrins as potential photosensitizers for antimicrobial photodynamic therapy, *J. Med. Chem.* 53 (21) (2010) 7796–7803.
- [37] H. Li, T.J. Jensen, F.R. Fronczek, M.G.H. Vicente, Syntheses and properties of a series of cationic water-soluble phthalocyanines, *J. Med. Chem.* 51 (3) (2008) 502–511.
- [38] A.P.D. Ribeiro, M.C. Andrade, V.S. Bagnato, C.E. Vergani, F.L. Primo, A.C. Tedesco, A.C. Pavarina, Antimicrobial photodynamic therapy against pathogenic bacterial suspensions and biofilms using chloro-aluminum phthalocyanine encapsulated in nanoemulsions, *Lasers Med. Sci.* 30 (2) (2015) 549–559.
- [39] Y. Gao, B. Mai, A. Wang, M. Li, X. Wang, K. Zhang, Q. Liu, S. Wei, P. Wang, Antimicrobial properties of a new type of photosensitizer derived from phthalocyanine against planktonic and biofilm forms of *Staphylococcus aureus*, *Photodiagn. Photodyn. Ther.* 21 (2018) 316–326.
- [40] J. Długaszewska, W. Szczolko, T. Koczorowski, P. Skupin-Mrugalska, A. Teubert, K. Konopka, M. Kucinska, M. Murias, N. Düzgüneş, J. Mielcarek, Antimicrobial and anticancer photodynamic activity of a phthalocyanine photosensitizer with N-methyl morpholiniummethoxy substituents in non-peripheral positions, *J. Inorg. Biochem.* 172 (2017) 67–79.
- [41] V. Mantareva, V. Kussovski, I. Angelov, D. Wöhrle, R. Dimitrov, E. Popova, S. Dimitrov, Non-aggregated Ga (III)-phthalocyanines in the photodynamic inactivation of planktonic and biofilm cultures of pathogenic microorganisms, *Photochem. Photobiol. Sci.* 10 (1) (2011) 91–102.
- [42] V. Mantareva, V. Kussovski, I. Angelov, E. Borisova, L. Avramov, G. Schnurpfeil, D. Wöhrle, Photodynamic activity of water-soluble phthalocyanine zinc (II) complexes against pathogenic microorganisms, *Bioorg. Med. Chem.* 15 (14) (2007) 4829–4835.
- [43] M. Soncin, C. Fabris, A. Buseti, D. Dei, D. Nistri, G. Roncucci, G. Jori, Approaches to selectivity in the Zn (II)-phthalocyanine-photosensitized inactivation of wild-type and antibiotic-resistant *Staphylococcus aureus*, *Photochem. Photobiol. Sci.* 1 (10) (2002) 815–819.
- [44] J.B. Pereira, E.F. Carvalho, M.A. Faustino, R. Fernandes, M.G. Neves, J.A. Cavaleiro, N.C. Gomes, A. Cunha, A. Almeida, J.P. Tomé, Phthalocyanine thio-pyridinium derivatives as antibacterial photosensitizers, *Photochem. Photobiol.* 88 (3) (2012) 537–547.
- [45] L.M. Lourenço, A. Sousa, M.C. Gomes, M.A. Faustino, A. Almeida, A.M. Silva, M.G. Neves, J.A. Cavaleiro, A. Cunha, J.P. Tomé, Inverted methoxypyridinium phthalocyanines for PDI of pathogenic bacteria, *Photochem. Photobiol. Sci.* 14 (10) (2015) 1853–1863.
- [46] X. Wen, X. Zhang, G. Szewczyk, A. El-Hussein, Y.-Y. Huang, T. Sarna, M.R. Hamblin, Potassium iodide potentiates antimicrobial photodynamic inactivation mediated by rose bengal in vitro and in vivo studies, *Antimicrob. Agents Chemother.* 61 (7) (2017) e00467-17.
- [47] I. Scalise, E.N. Durantini, Synthesis, properties, and photodynamic inactivation of *Escherichia coli* using a cationic and a noncharged Zn (II) pyridyloxypthalocyanine derivatives, *Bioorg. Med. Chem.* 13 (8) (2005) 3037–3045.
- [48] O.L. Osifeko, M. Durmuş, T. Nyokong, Physicochemical and photodynamic antimicrobial chemotherapy studies of mono- and tetra-pyridyloxy substituted indium (III) phthalocyanines, *J. Photochem. Photobiol. A Chem.* 301 (2015) 47–54.
- [49] D. Dei, G. Chiti, M.P. De Filippis, L. Fantetti, F. Giuliani, F. Giuntini, M. Soncin, G. Jori, G. Roncucci, Phthalocyanines as photodynamic agents for the inactivation of microbial pathogens, *J. Porphyr. Phthalocyanines* 10 (03) (2006) 147–159.
- [50] I. Angelov, V. Mantareva, V. Kussovski, D. Wöhrle, E. Borisova, L. Avramov, In Improved antimicrobial therapy with cationic tetra- and octa-substituted phthalocyanines, in: 15th International School on Quantum Electronics: Laser Physics and Applications, International Society for Optics and Photonics, 2008, p. 702717.
- [51] V. Kussovski, V. Mantareva, I. Angelov, P. Orozova, D. Wöhrle, G. Schnurpfeil, E. Borisova, L. Avramov, Photodynamic inactivation of *Aeromonas hydrophila*

- by cationic phthalocyanines with different hydrophobicity, *FEMS Microbiol. Lett.* 294 (2) (2009) 133–140.
- [52] M.A. Di Palma, M.G. Alvarez, E.N. Durantini, Photodynamic action mechanism mediated by zinc (II) 2, 9, 16, 23-tetrakis [4-(N-methylpyridyloxy)] phthalocyanine in *Candida albicans* cells, *Photochem. Photobiol.* 91 (5) (2015) 1203–1209.
- [53] B.-Y. Zheng, M.-R. Ke, W.-L. Lan, L. Hou, J. Guo, D.-H. Wan, L.-Z. Cheong, J.-D. Huang, Mono- and tetra-substituted zinc (II) phthalocyanines containing morpholinyl moieties: synthesis, antifungal photodynamic activities, and structure-activity relationships, *Eur. J. Med. Chem.* 114 (2016) 380–389.
- [54] B. Pucelik, R. Paczyński, G. Dubin, M.M. Pereira, L.G. Arnaut, J.M. Dąbrowski, Properties of halogenated and sulfonated porphyrins relevant for the selection of photosensitizers in anticancer and antimicrobial therapies, *PLoS One* 12 (10) (2017) e0185984.
- [55] E. Reddi, M. Ceccon, G. Valduga, G. Jori, J.C. Bommer, F. Elisei, L. Latterini, U. Mazzucato, Photophysical properties and antibacterial activity of meso-substituted cationic porphyrins, *Photochem. Photobiol.* 75 (5) (2002) 462–470.
- [56] M.M. Awad, A. Tovmasyan, J.D. Craik, I. Batinic-Haberle, L.T. Benov, Important cellular targets for antimicrobial photodynamic therapy, *Appl. Microbiol. Biotechnol.* 100 (17) (2016) 7679–7688.
- [57] K. Li, Y.-Y. Zhang, G.-Y. Jiang, Y.-J. Hou, B.-W. Zhang, Q.-X. Zhou, X.-S. Wang, A bivalent cationic dye enabling selective photo-inactivation against Gram-negative bacteria, *Chem. Commun.* 51 (37) (2015) 7923–7926.
- [58] Z. Xu, Y. Gao, S. Meng, B. Yang, L. Pang, C. Wang, T. Liu, Mechanism and in vivo evaluation: photodynamic antibacterial chemotherapy of lysine-porphyrin conjugate, *Front. Microbiol.* 7 (2016) 242.
- [59] S. Makhseed, M. Machacek, W. Alfidly, A. Tuhl, M. Vinodh, T. Simunek, V. Novakova, P. Kubat, E. Rudolf, P. Zimcik, Water-soluble non-aggregating zinc phthalocyanine and in vitro studies for photodynamic therapy, *Chem. Commun.* 49 (95) (2013) 11149–11151.
- [60] S.G. Telfer, T.M. McLean, M.R. Waterland, Exciton coupling in coordination compounds, *Dalton Trans.* 40 (13) (2011) 3097–3108.
- [61] L. Huang, G. Szweczyk, T. Sarna, M.R. Hamblin, Potassium iodide potentiates broad-spectrum antimicrobial photodynamic inactivation using Photofrin, *ACS Infect. Dis.* 3 (4) (2017) 320–328.
- [62] A. Ogunsipe, J.-Y. Chen, T. Nyokong, Photophysical and photochemical studies of zinc (II) phthalocyanine derivatives—effects of substituents and solvents, *New J. Chem.* 28 (7) (2004) 822–827.
- [63] J.-W. Hofman, F. Van Zeeland, S. Turker, H. Talsma, S.A. Lambrechts, D.V. Sakharov, W.E. Hennink, C.F. van Nostrum, Peripheral and axial substitution of phthalocyanines with solketal groups: synthesis and in vitro evaluation for photodynamic therapy, *J. Med. Chem.* 50 (7) (2007) 1485–1494.
- [64] V. Chauke, M. Durmuş, T. Nyokong, Photochemistry, photophysics and nonlinear optical parameters of phenoxy and tert-butylphenoxy substituted indium (III) phthalocyanines, *J. Photochem. Photobiol. A Chem.* 192 (2–3) (2007) 179–187.
- [65] J.M. Dąbrowski, B. Pucelik, M.M. Pereira, L.G. Arnaut, G. Stochel, Towards tuning PDT relevant photosensitizer properties: comparative study for the free and Zn²⁺ coordinated meso-tetrakis [2, 6-difluoro-5-(N-methyl-sulfamoyl) phenyl] porphyrin, *J. Coord. Chem.* 68 (17–18) (2015) 3116–3134.
- [66] T. Nyokong, V. Ahsen, *Photosensitizers in Medicine, Environment, and Security*, Springer Science & Business Media, 2012.
- [67] L. Huang, Y. Xuan, Y. Koide, T. Zhiyentayev, M. Tanaka, M.R. Hamblin, Type I and Type II mechanisms of antimicrobial photodynamic therapy: an in vitro study on gram-negative and gram-positive bacteria, *Lasers Surg. Med.* 44 (6) (2012) 490–499.
- [68] A. Preuss, L. Zeugner, S. Hackbarth, M. Faustino, M. Neves, J. Cavaleiro, B. Roeder, Photoinactivation of *Escherichia coli* (SURE 2) without intracellular uptake of the photosensitizer, *J. Appl. Microbiol.* 114 (1) (2013) 36–43.
- [69] T. Maisch, S. Hackbarth, J. Regensburger, A. Felgenträger, W. Bäumler, M. Landthaler, B. Röder, Photodynamic inactivation of multi-resistant bacteria (PIB)—a new approach to treat superficial infections in the 21st century, *JDDG J. der Deutschen Dermatol. Gesellschaft* 9 (5) (2011) 360–366.
- [70] U. Food, D. Administration, Class II Special Controls Guidance Document: Antimicrobial Susceptibility Test (AST) Systems; Guidance for Industry and FDA, US Food and Drug Administration, Rockville, MD, 2003.
- [71] F.A. Schaberle, Assessment of the actual light dose in photodynamic therapy, *Photodiagn. Photodyn. Ther.* 23 (2018) 75–77.
- [72] Ü. İsci, M. Beyreis, N. Tortik, S.Z. Topal, M. Glueck, V. Ahsen, F. Dumoulin, T. Kiesslich, K. Plaetzer, Methylsulfonyl Zn phthalocyanine: a polyvalent and powerful hydrophobic photosensitizer with a wide spectrum of photodynamic applications, *Photodiagn. Photodyn. Ther.* 13 (2016) 40–47.
- [73] A. Spaeth, A. Graeler, T. Maisch, K. Plaetzer, CureCuma—cationic curcuminoids with improved properties and enhanced antimicrobial photodynamic activity, *Eur. J. Med. Chem.* 159 (2018) 423–440.
- [74] M.R. Hamblin, D.A. O'Donnell, N. Murthy, K. Rajagopalan, N. Michaud, M.E. Sherwood, T. Hasan, Polycationic photosensitizer conjugates: effects of chain length and Gram classification on the photodynamic inactivation of bacteria, *J. Antimicrob. Chemother.* 49 (6) (2002) 941–951.
- [75] Z. Chen, S. Zhou, J. Chen, L. Li, P. Hu, S. Chen, M. Huang, An effective zinc phthalocyanine derivative for photodynamic antimicrobial chemotherapy, *J. Lumin.* 152 (2014) 103–107.
- [76] J.M. Dąbrowski, M.M. Pereira, L.G. Arnaut, C.J. Monteiro, A.F. Peixoto, A. Karocki, K. Urbańska, G. Stochel, Synthesis, photophysical studies and anticancer activity of a new halogenated water-soluble porphyrin, *Photochem. Photobiol.* 83 (4) (2007) 897–903.